A Low-Cost Handheld Impedimetric Biosensing System for Rapid Diagnostics of SARS-CoV-2 Infections

Giancarlo Ayala-Charca, *Member, IEEE*, Razieh Salahandish, Mahmood Khalghollah, *Graduate Student Member, IEEE*, Deniz Sadighbayan, Fatemeh Haghayegh, Amir Sanati-Nezhad, and Ebrahim Ghafar-Zadeh, *Senior Member, IEEE*

***Abstract*—Current laboratory diagnostic approaches for virus detection give reliable results, but they require a lengthy procedure, trained personnel, and expensive equipment and reagents; hence, they are not a suitable choice for home monitoring purposes. This paper addresses this challenge by developing a portable impedimetric biosensing system for the identification of COVID-19 patients. This sensing system has two main parts: a throwaway two-working electrode (2-WE) strip and a novel read-out circuit, specifically designed for simultaneous signal acquisition from both working electrodes. Highly reliable electrochemical signal tracking from multiplex immunosensors provides a potential for flexible and portable multi-biomarker detection. The electrodes' surfaces were functionalized with SARS-CoV-2 Nucleocapsid Antibody enabling the selective detection of Nucleocapsid protein (N-protein) along with self-validation in the clinical nasopharyngeal swab specimens. The proposed programmable highly sensitive impedance read-out system allows for a wide dynamic detection range, which makes the sensor capable of detecting N-protein concentrations between 0.116 and 10,000 pg/mL. This lightweight and economical read-out arrangement is an ideal prospect for being mass-produced, especially during urgent pandemic situations. Also, such an impedimetric sensing platform has the potential to be redesigned for targeting not only other infectious diseases but also other critical disorders.**

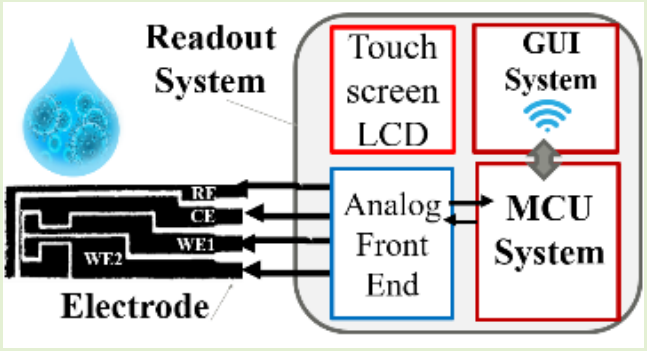

***Index Terms*— SARS-CoV-2, biosensor, impedance measurement, dual electronic read-out system.**

I. Introduction

AN UNIDENTIFIED strain of coronavirus -now called Severe Acute Respiratory Syndrome Coronavirus-2 (SARS-CoV-2)- was first recognized in early January 2020, which had an enormous impact on every aspect of people's lives from daily communications to considerable losses [1]. Even though several effective vaccines have been rolled out all over the world and some efficient drugs have been developed against this infection, the virus is continuing to survive in the shape of new variants [2]. Therefore, as specified by the Director-General of the World Health Organization (WHO), "Test every suspected case," is the key for deteriorating the spread [3]. Besides, the clinical symptoms of COVID-19 are very similar to other respiratory tract-related diseases like influenza [4]. So, developing a sensitive, portable and selective test has been vital for differentiating the actual COVID-19 patients without violating the social distancing requirements.

From the onset of the pandemic, a large number of portable COVID-19 testing devices have been proposed for detecting the COVID-19-related biomarkers such as viral antigens, host antibodies, and viral genetic material [5]. Various biosensing techniques including electrochemical, Lateral Flow, and field-effect transistor (FET) has recently been used in these portable devices for the quantification of SARS-CoV-2 [6]. Among these, the rapid U.S. Food and Drug Administration (FDA) approved Lateral Flow technique [7] has been used for Coronavirus detection [8]. Despite the great advantages of this portable sensing device for detecting most people at risk of transmitting Covid-19, still this method is not quantitative and

Manuscript received 3 May 2022; accepted 25 May 2022. Date of publication 13 July 2022; date of current version 15 August 2022. This work was supported in part by the Canadian Institutes of Health Research (CIHR); in part by the Natural Sciences and Engineering Research of Canada (NSERC) through Rapid COVID-19; in part by the Canada Research Chair, NSERC CREATE Wearable Technology Research and Collaboration (We-TRAC) Training Program through York University, University of Calgary, and CMC—Microsystems, Canada, under Project CREATE/511166-2018. The associate editor coordinating the review of this article and approving it for publication was Prof. Irene Taurino. *(Corresponding author: Ebrahim Ghafar-Zadeh.)*

This work involved human subjects or animals in its research. Approval of all ethical and experimental procedures and protocols was granted by the University of Calgary's Ethics Board, Alberta, Canada, under Ethics No. REB20-1032.

Please see the Acknowledgment section of this article for the author affiliations.

Digital Object Identifier 10.1109/JSEN.2022.3181580

it cannot be employed for the assessment of disease severity. In general, the quantitative optical sensing methods are costly and laborious and not suitable for home monitoring purposes [9]. Among different methodologies suitable for portable COVID-19 sensing purposes, electrochemical-based devices are one of the best alternatives for quantitative COVID-19 detection owing to their accurate and low-cost single-use sensing electrodes and reusable readout out systems [10], [11]. Their small sizes enable the fabrication of miniaturized sensors and mini-potentiostats that can be used on-site [12]. Thus, the risk of infection spread in health centers decreases considerably [13], [14]. In addition, their development is closely linked to the improvements in the cost-effective manufacture of microelectronic circuits and uncomplicated interface with standard read-out processing, all of which set the stage for their popularity among biosensor researchers, in particular during the urgent pandemic where the shortage of electronic components is of concern [15].

Among various electrochemical techniques, impedance-based sensors have been reported to show high stability over a wide range of applied frequencies [16]–[18]. Since these label- free sensing methods can rapidly produce a signal when an interaction occurs between an immobilized Biorecognition Element (BRE) and a target biomolecule such as SARS-CoV-2 nucleocapsid protein in the sample, which can be utilize for real-time monitoring of the electrochemical interactions [14] It is noteworthy, a smartphone can be used as reliable graphical user interface (GUI) system connected to biosensors [12], [26], [27] in order to read, display, transfer and/or save measurement data in the cloud for further processing purposes, however, in this paper, we propose an stand-alone impedance based biosensor with required wireless and other features (see Section III) for the quantitative detection of SARS-CoV-2.

The remainder of this paper covers the related works in the literature and challenges in section II, the proposed sensing platform in section III, and the electrochemical characterization and clinical sample testing results in section IV, followed by a conclusion. in section V.

II. Related Works

Up until now, several research studies have been conducted on developing COVID-19 biosensors by measuring the concentration of spike (S1) protein [19]–[21], [28]–[30] and nucleocapsid (N) protein [23], [31]. As an example, Fabiani *et al.* reported sensing assay using magnetic beads combined with SPCE for measuring N and S protein with an LoD of ∼8ng/mL and an LR of 10-100 ng/mL [20]. In this direction, various sensing electrodes using fluorine-doped tin oxide electrode (FTO) with gold nanoparticle (AuNPs), electroless nickel immersion gold (ENIG) finish Printed Circuit Boards (PCBs) or Molecularly imprinted polymers (MIPs) were reported to achieve lower LoD and higher LR [19]–[21], [28], [29]. As seen in Table I, these methods require cumbersome readout systems such as commercially available (CA) benchtop or handheld devices [19]–[21], [28], [29] and less attention has been paid to developing custom-made (CM) readers for this purpose. Among these few works, Perdomo *et al.* reported the development of a low-cost CM impedimetric readout system for detecting COVID-19 using screen-printed carbon working electrodes with a layer of Ag/AgCl. They successfully demonstrated a low LoD equal to 1.065 fg/mL [19], but in a narrow range of 1 to 20 fg/mL with a response and electrode's preparation time of higher than 10 min. In this work, we address the challenge of developing a low-cost biosensor for accurately measuring the concentration of N protein in a wide linear range. Furthermore, the proposed CM impedimetric readout system can simultaneously record the impedance changes of two WEs.

TABLE I
ELECTROCHEMICAL-BASED PORTABLE BIOSENSORS FOR DETECTING COVID-19 USING N AND P PROTEINS' BIOMARKERS

T.Q.	CM	$CA	BK	Time (min)	LOD (fg/mL)	MLR (fg/mL)	#E	Ref.
EIS	Y	250	S	10	1.065	20	1	[19]
DPV	N	>3k	N	~185	$8x10^6$	10^9	1	[20]
DPV	N	>1k	S	>15×60	10^5	$2×10^7$	1	[21]
V	Y	NA	S	30	17100	$190×10^9$	1	[22]
DPV	N	>1k	S	15	630	6882	1	[23]
EIS	Y	150	N	15	116	10^7	2	This study

III. Biosensing Electrodes

In this study, for evaluating the performance of the developed read-out system, we have incorporated 2-WE screen-printed strips, purchased from Criticare Dx, Canada. The electrodes employ a bio-ready technology, meaning that they are produced from carboxyl-rich nanomaterial contained ink, composed of poly (3, 4-ethylenedioxythiophene) polystyrene sulfonate (PEDOT:PSS) conductive polymers and reduced graphene oxide nanosheets in a base carbon matrix, which provides ample binding sites for immobilizing the biorecognition elements. The amended surface contains carboxyl (–COOH) groups allowing for covalent bonding of antibodies via amide bonds, without any prior functionalization steps. More precisely, the carboxyl groups interact with the free amino groups of the antibody, to generate a covalent amide bond. All working, reference, and counter electrodes are fabricated using the same material. Upon obtaining the electrodes, based on the specific experiments, each of the working electrodes was drop-cast with 50 μg/mL of the SARS-CoV-2 antibody (SARS-CoV-2 Nucleocapsid Antibody (HC2003), Genscript, USA), and incubated at room temperature for 1 hr, to increase the immobilization reaction kinetics [32], [33], and after that maintained in 4°C overnight. To track the capability of the bi-potentiostat in distinguishing the antibody/antigen immunoreaction, the immobilized electrodes were first passivated using 0.005% of bovine serum albumin (BSA, ChemCruz, #sc-2323, USA), before exposing the immunosensor to standard concentrations of nucleocapsid protein of SARS-CoV-2 (#Z03488, Genscript, USA), from 1 pg/mL to 10 ng/mL. All biological solutions were prepared in 1X phosphate-buffered saline (PBS 1X, Growcells, USA, pH = 7.4, #MRGF-6230). The mentioned stepwise

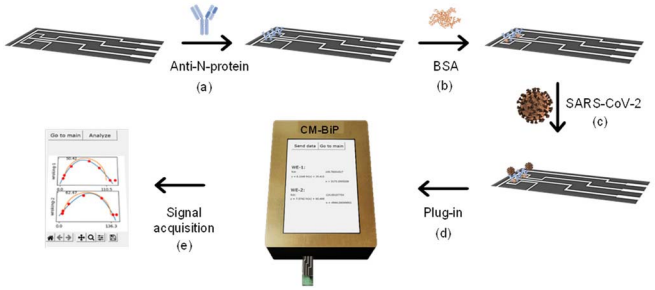

Fig. 1. An illustration of the step-by-step preparation of immunosensor using bio-ready two-working electrode strips, (a) antibody-immobilization, (b) bovine serum albumin (BSA) blocking, (c) virus surface protein (N-protein) detection (d) sensor connection to the custom-made bi-potentiostat (CM-BiP), and ultimate (e) signal generation and acquisition using CM-BiP system.

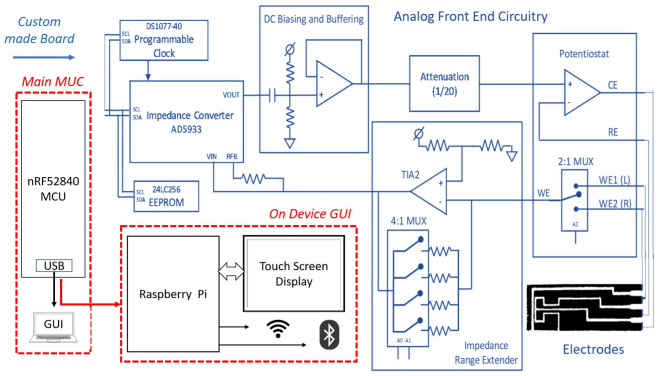

Fig. 2. Illustration of proposed system design. Analog/digital custom-made interface (blue) featuring the potentiostat, attenuator, buffer, impedance converter, range extender and other circuitries for power supply etc. Microcontroller and microprocessor systems (red) are used for the control of the interface system and for graphical user interface (GUI) purposes.

immunosensor preparation process is depicted in Fig. 1, and as shown, the prepared immunosensor is then proceeded for detecting the viral particles, through expressing signal changes associated with alterations in surface charge transfer resistance. Based on the manufacturer guidelines, the strips are compatible with a commercially available connector (Molex, 0472861001), which was used for electrical connection to the read-out system. As for the electroactive medium for generating the electrochemical signals, 2.5 mM of the $[Fe(CN)_6]^{3-/4-}$ (#702587, Sigma, USA) in PBS was used. SARS-CoV-2 Spike protein (S1) (Genscript Inc., USA, #T80202), as well as Immunoglobulin G (IgG) from human serum (Sigma, USA, #I4506) were utilized for selectivity evaluation studies.

IV. Read-Out System

This section covers the design metrics, the techniques used in the development of circuits and systems.

A. System Design

Herein, we put forward the system of design satisfying the design matrices described in section A. The proposed read-out system consists of an analog front-end circuitry that applies a sinewave voltage V_{in} on WE1 or WE2 electrodes, then detects and transduces the current flowing through the unknown impedance (Z) to the impedance converter's IC [34]. This chip calculates Z by generating V_Z and detecting the I_Z. The operation of this converter is controlled by the digital devices including nRF52840 microcontroller unit (MCU) [35], 24LC256 memory [36], and a DS1077-40 programmable clock [37]. This MCU-based digital system is also programmed to tune the analog front-end to select and accurately operate in each one of 7 critical frequencies. A graphical user interface (GUI) is also considered in this system as shown in Fig. 2. The graphical user interface allows for initializing and communicating with the MCU to control other aforementioned digital devices. Moreover, the MCU sends the instructions to generate the frequency clocks from the Programmable Clock to the Impedance Converter, retrieve the calibration parameters from EEPROM when necessary, and allow the Impedance Converter module to operate and apply the signals needed for this application. Each component is further explained, after putting forward the design's metrics, in the following subsection.

1) Design Metrics: The main design features of the proposed readout system are as follows.

Multiplexing: This system allows the recording of impedance from two WEs on the same electrode. This configuration potentially allows for simultaneous detection of two different bio-analytes. Both working electrodes operate independently with high reproducibility and sensitivity.

Range of Frequencies: In this design, at the first stage, the functionalized sensing electrodes were electrically and electrochemically characterized and then tested using different concentrations of target SARS-CoV-2 N-protein, by Metrohm potentiostat (PGSTAT204) impedance spectroscopy as described in section V. As per these experiments, the selected range of frequencies covers 1 Hz to 5 kHz and the amplitude of excitation voltage is 10 mV.

Impedance auto-ranging: As per experimental results using the standard Metrohm potentiostat, the impedance values of the proposed biosensor vary between 100 Ω – 1 MΩ. in order to measure the required target molecules' concentrations (0.116 pg/mL to 10 ng/mL). This wide range of impedance is divided into multiple ranges and selected automatically using the programmed microcontroller.

Reduced response time: In the proposed design, instead of sweeping a whole range of frequencies that takes more than 15 minutes, this hand-held read-out system assesses the impedance spectrum using 7 logarithmically spaced points chosen over 1400 Hz to 1 Hz for both working electrodes in less than 2 min with an acceptable accuracy as demonstrated and discussed in section IV.

Discrete electronic components: One of the goals of this work was to develop a reliable design using off-the-shelf electronic components that would be commercially available during an urgent pandemic situation.

2) Microcontroller: The selected MCU breakout is the SparkFun Pro nRF52840 Mini [38] based on the nRF52840 (Nordic Semiconductor) with ARM Cortex-M4 32-bit processor

(64 MHz, 1 MB flash, 256 kB RAM), and 2.4 GHz Bluetooth low-energy (BLE) radio. The USB interface allows for programming the MCU, powering the unit, and communicating through UART. The breakout can also be powered by a Lithium-Polymer (LiPo) battery and charged using the same USB interface. The firmware was developed using Arduino IDE and Adafruit nRF52 Arduino core libraries. The aforementioned features along with low cost (∼$5) are the main reason for selecting this microcontroller.

3) Impedance Converter: In this design, we selected AD5933 16SSOP (Analog Devices) as an accurate and reliable impedance converter. To date many papers have reported the design and implementation of impedance spectroscopy using AD5933 [11], [39]–[43]. Herein we propose a novel custom-made core-AD5933 impedance readout system featuring the aforementioned design matrices for developing a low cost, reliable, accurate, quantitative COVID-19 detection. This integrated circuit (IC) has a 27-bit phase accumulator direct digital synthesis (DDS) and digital to analog converter (DAC) to generate the sinusoidal signals along with programmable gain amplifiers (PGA) to set four different output voltages and their respective DC bias (V_{BIAS}). This feature of the device allows us to develop a novel custom-made multi-range impedance reader as shown in the circuitry in the next section. The receiving stage of this chip converts the current into voltage using an internal trans-impedance aamplifier (TIA) in a voltage follower configuration, followed by a PGA, a low pass filter (LPF), and a 12-bit analog to digital converter (ADC). This architecture enables an internal 1024-point discrete Fourier transformation (DFT) engine to accurately and reliably process the data and return the real (Re) and imaginary (Im) components of the impedance. To control the impedance converter, we used the AD5933 Arduino Library developed by Michael Meli [44] and modified by Brian Millier [45]. We updated the library with a function to select the system clock, use it for frequencies lower than 1 kHz, and parametrize the start frequency and increment frequency functions, given that they depend not only on the internal oscillator but also on the external master clock (MCLK) signal.

4) Programmable Clock: The clock for the DDS of the impedance converter is supplied through either an internal oscillator (16.776 MHz) or an external source, a master clock (MCLK). According to the datasheet using the internal clock, the sampling frequency of the ADC is 1/16 of the system clock. Considering the need for 1024 samples for the DFT calculation of one frequency point, a factor of 1/1024 is applied for the final frequency resolution. This implies working with the frequency of 16.667 MHz with the ADC sampling frequency of 1.049 MHz and the DFT resolution of 1.024 kHz. To be able to analyze signals lower than 1 kHz, the system clock needs to be scaled down. In this case, the DS1077L single supply low-jitter programmable oscillator allows for generating signal clocks down to 4.87 kHz suitable for this purpose [46]. In addition, the excitation signal needs to have an integer number of cycles over the 1024 sample interval, otherwise, a spectral leakage may appear and introduce errors in the impedance calculation. All these considerations were taken into account to select proper external MCLK frequency clocks.

5) Memory: To store the calibration parameters of the system, such as gain factors and system phases, an external I^2C EEPROM (24LC256, 32kB) is used. The data in the memory is allocated in two main blocks, each of 7168 bytes, named calibration gains and calibration phases. Each memory block contains the data organized in five memory segments of 1024 bytes. Each segment contains calibration data for the whole frequency range, in this case, 75 points distributed from 1 Hz to 5000 Hz, expandable to higher frequencies. The frequency range is divided into four groups, called frequency bands (FB). All the values are stored in 32 bits IEEE floating-point format, therefore every gain factor or system phase occupies 4 bytes in memory.

6) User Interaction System: The read-out system was additionally integrated with the single-board computer Raspberry pi and a 3.5-inch liquid crystal display (LCD), to provide an easy and friendly user interface, with the capability for wireless internet, cloud storage, and remote analysis (Web-based Application). The application and all the analysis modules could be updated remotely. The Raspberry pi computer communicates with the EIS read-out system through a serial port and provides a friendly graphical user interface through the LCD touchscreen display that is controlled via General Purpose Input/Output (GPIO) pins. A python-based application has been developed to run under a customized Raspbian OS to make data collection, storage, and data analysis easier, while the GUI provides instructions to collect the sample, run the test and show the results.

The general procedure is as follows. Once the application is launched, the user logs into the device to obtain a user ID to allow saving the data in the cloud. Then a sample number is requested for the data processing and retrieving. The sample is inserted into the device and the start button initiates the EIS measurement. Once the EIS process is finished, the EIS data is used to fit the equivalent electrical model and determine the R_{ct} (charge transfer resistance). Finally, the extracted R_{ct} is used in the exponential relationship to find the N-protein concentration in pg/mL. The results are plotted and saved in the device to send data to the cloud for healthcare data collection, and further analysis.

B. Analog Circuit Design

In the Analog Front-End, an RC high pass filter (Fig. 3a) is used to re-bias the DC level (1.5V) of the output voltage [47]. To extend the low-frequency limit to 1 Hz, the value of the coupling capacitor was increased to 20 uF providing a longer time constant for the lowest frequency (1 Hz). The output impedance was reduced with an op-amp buffer; in this case, we used the AD8608 quad ($Z_{out} \sim 1\Omega$) (Fig. 3c). Due to the requirement of working with biological samples, we need to attenuate the excitation voltage down to 10 mV (Fig. 3d). For this purpose, a combination of an inverting buffer and an inverting amplifier helps to perform the task while keeping the signal phase and DC bias constant. To complement the circuitry, the potentiostat (Fig. 3e) is implemented with an additional op-amp that applies the output signal in the CE

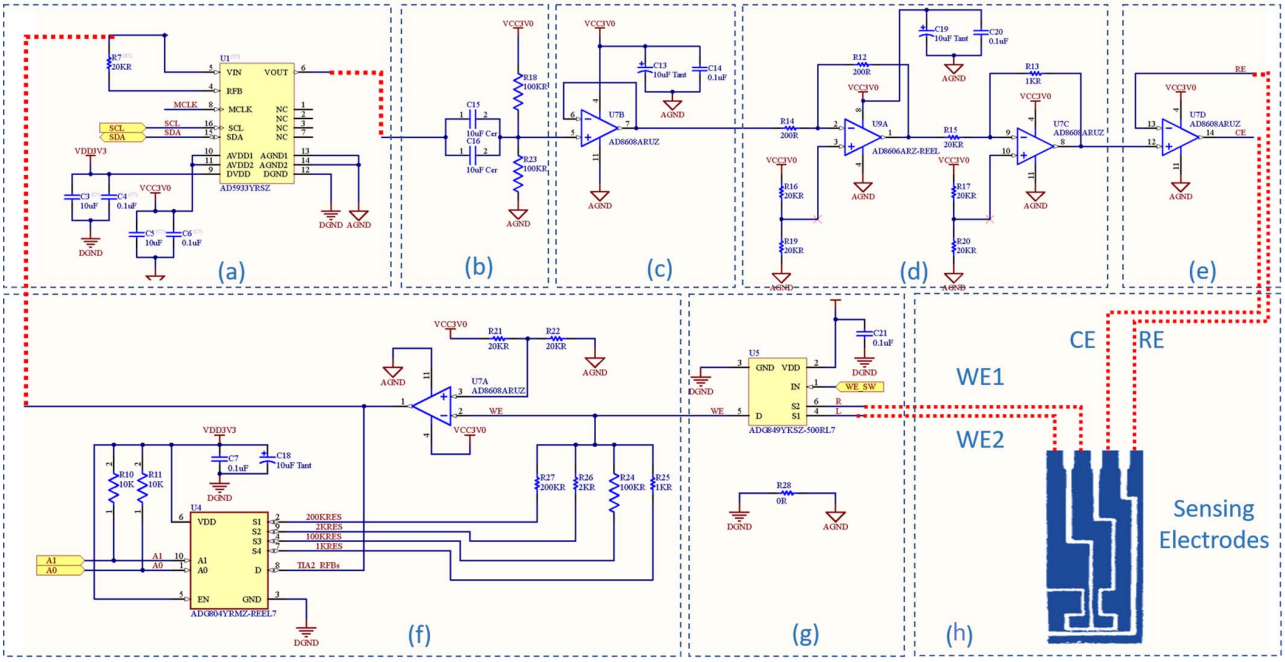

Fig. 3. Custom designed analog circuitries consisting of (a) excitation signal generator/impedance converter, (b) High pass filter with input from impedance converter, (c) buffer, (d) attenuator, (e) potentiostat, (f) transimpedance amplifier and multiplexer for selection of TIA feedback resistor, (TIA) (g) working electrode section switch, (h) electrode.

and maintains the RE at the same potential via the negative terminal of the opamp.

For multiplexing the two-working electrode (WE1, WE2) in the screen-printed electrodes, the single-pole double-throw (SPDT) 2:1 multiplexer (ADG849) was used (Fig. 3g). While keeping the same bias voltage at the WE, the current that flows from the counter electrode (CE) through the sample to the WE is converted into voltage and amplified with an external TIA (Fig. 3f). Depending on the size of the unknown impedance, the ADG804 4:1 multiplexer (Fig. 3f) allows for selecting the proper feedback resistor for the desired gain to extend the impedance range and return the signal to the converter (Fig. 3a) for the impedance calculation. The TIA and the array of feedback resistors constitute an impedance range extender block. The possible gains allow reaching 100 or 500 mVpp at the input of the internal ADC of the impedance converter to operate a different range of impedances.

C. Serial Communication

The communication between the MCU and the impedance converter is implemented through the standard I^2C interface with a 100 kHz clock. The default system clock for the Impedance converter AD5933 is 16.776 MHz. However, the I^2C clock (SCL) needs to be slowed down to frequencies lower than the MCLK frequency to provide enough time for the conversion before transmitting the data through the serial interface. To do this, we edited the two-wire interface (TWI) master clock frequency and TWIM frequency register (nrf52840 bitfields.h and nrf52 bitfields.h library files and set the clock function at Wire_nRF52.cpp file), defining new frequencies such as 50 kHz, 12.5 kHz, and 6.25 kHz. Although the resulting actual rates are not exactly the target frequencies, they are close enough and conveniently lower than the external clock MCLK.

D. Practical Considerations in PCB Design

The printed circuit board (PCB) was designed in Altium Designer software, taking careful consideration for the mixed-signal system (Fig. 4b-4c). In the design, the PCB ground plane is split into an analog plane (AGND) and a digital plane (DGND) to reduce the noise coupled from digital circuits into the analog signals. Analog and digital components were separated and their corresponding signal traces were placed right above their respective ground planes. In this way, the signals return to their ground planes by vias. In this mixed-signal PCB, we also have components that have analog and digital rail connections, such as the impedance converter (U1: AD5933), SPDT 2:1 multiplexer (U5: ADG849), and 4:1 Multiplexer (U4: ADG804). They were placed in a way that no traces cross the split in the plane in order to avoid ground loops. Finally, the split planes were joined together underneath the AD5933, with a zero-ohm resistor (R28), to make the system "star" ground in a single point, as a suggested solution by 'Analog Devices' for mixed-signal systems.

Because the MCU breakout has a Sparkfun Qwiick connector (4-pin JST) with 2.2K Ohm pull-up resistors on-board that is not suitable for our I2C bus (4.7 kΩ), the pin hardware definitions were modified (variant.h library pinout definitions), thanks to the expansive pin multiplexing capability of the nRF52840's Cortex-M4. Given that the total cost of elements

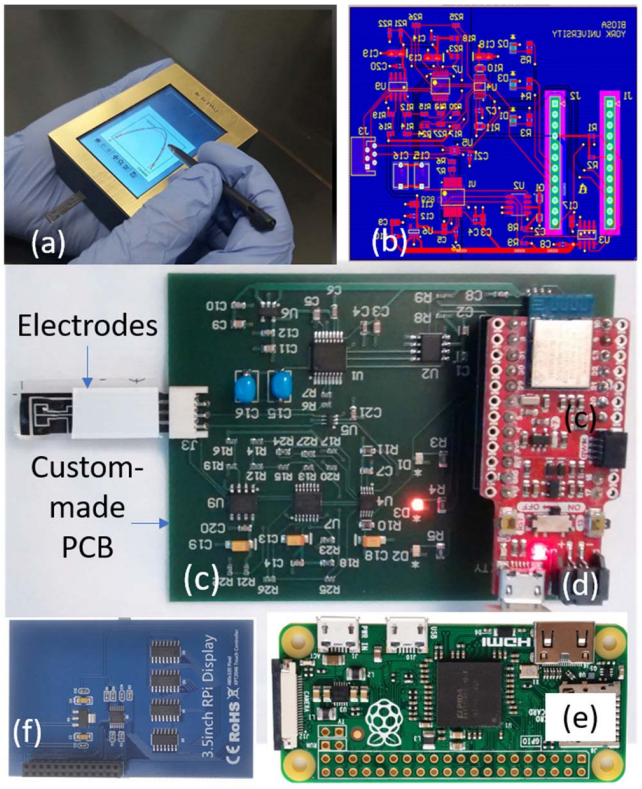

Fig. 4. Proposed read-out System: (a) whole packaged system, (b) Printed Circuit Board Layout using Altium Designer Software, (c) custom-made PCB, (d) main MCU, (e) RPi board and (f) LCD board.

TABLE II
LIST AND COST OF COMPONENTS USED IN THE CUSTOM-MADE PCB

ELEMENT	DETAIL	Q.	$
C13, 18-19	Capacitor, Tantalum, 10 uF, +/- 10%,	3	$0.68
C15, C16	Ceramic Capacitor 10uF ±10% 50V	2	$1.70
C1, ETC	CAP CER 0.1UF 50V X7R 0603 and etc.	1	$0.13
D1	LED YELLOW CLEAR 0805 SMD	1	$0.57
D2	LED Red 630nm 18deg Clear 0805	1	$0.57
D3	LED ORANGE CLEAR 0805 SMD	1	$0.57
J1, J2	CONN HDR 12POS 0.1 TIN PCB	2	$0.99
J3	1.0 mm Pitch FFC Connector	1	$0.62
R18, 23, 24	Surface Mount Metal Film Resistor	3	$0.92
R3, ETC	RES SMD 10KΩ 1% 1/16W 0603 and etc.	25	~$0.22
U1	1 MSPS, 12-Bit Impedance Converter	1	$45.85
U2	IC, ECON OSC/DIVIDER, 40MHZ	1	$4.42
U3	256Kbit, 400kHz, I2C Serial EEPROM	1	$1.02
U4	IC MULTIPLEXER 4X1 10MSOP	1	$4.39
U5	3 V / 5 V CMOS 0.5 Ohm SPDT / 2:1 Mux	1	$2.63
U6	150 mA CMOS Linear Regulator	1	$1.35
U7	Quad Channel Wide Bandwidth OPMP	1	$6.15
U9	2 Channel Wide Bandwidth OPAMP	1	$4.59
TOTAL	All components of Analog circuits	63	$80.25

(see Table II) is less than ~$81 from Digi-Key distributer, the mass production of this device incorporated considering the cost of manufacturing PCB, GUI and assembly of devices should not exceed $150 which is a very cost-effective solution compared with other commercially available multi-thousand dollars portable impedance spectroscopy devices such as PalmSense impedance readers [20]–[23].

TABLE III
EQUIVALENT CIRCUITS EXTRACTED BY THE PROPOSED DEVICE AND AUTOLAB POTENTIOSTAT METROHM AT TWO DIFFERENT RANGES OF FREQUENCIES

	Proposed device (D)		*Metrohm(M)*	
F (Hz)	1-1400	5-5000	1-1400	5-5000
C(F)	30.0E-9	30.5E-9	30.2E-9	29.9E-9
R(Ω)	4128.9	3995.7	3510	3430
R_{ct}(Ω)	27.14E+3	25.69E+3	25.3E+3	24.8E+3

E. Calibration

The read-out system was calibrated with 0.1% precision metal film resistors (reference resistors). For the calibration, the CE and RE were short-circuited and the corresponding feedback resistor was selected to calculate the calibration Gains Factors and calibration System Phases, for five different impedance ranges. The procedures to estimate those values are as explained in the impedance converter datasheet [39]. Calibration factors were stored in the EEPROM for easy and fast access, for the whole frequency span (1 Hz – 5 kHz); in a way that the system does not need to re-calibrate at every measurement for each frequency point, and calibration data remains in the device.

V. RESULTS

A. Implementation Results

As seen in Fig. 4a, a package was prepared by integrating the read-out system with a data visualization unit (LCD), as well as a computation unit (MCU) and single-board computer (SBC). The weight of this prototype is about 200g that become even lighter in the final products by combining the Arduino and GUI and custom-made electronic interface boards on a single board. The package adds to the features offered by the potentiostat including processing the frequency response analysis (FRA) signals, calculating the R_{ct} values, obtaining the concentration results based on the fitted calibration curve, and showing the results.

B. Electrical Characterization

Functional tests were performed with 2.5 mM ferricyanide-ferrocyanide $K_3Fe(CN)_6/K_4Fe(CN)_6$ redox solution. For this purpose, a python program was developed for the communication between the read-out system and the computer. The impedance spectrum over two different ranges of frequencies (1-1400 Hz, 5-5000 Hz) was obtained in 7 logarithmically spaced points. Using the experimental data and the EIS Spectrum Analyser free software, the Nyquist plots and the equivalent circuits were obtained as seen in Fig. 5 and Table III. The equivalent circuit can be used to obtain R_{ct}. The variation of R_{ct} as a function of analytes including the SARS-CoV-2 N- protein is the main goal of this work.

The tests were validated with the Autolab PGSTAT204 from Metrohm, with FRA32M EIS module, and NOVA software. The test was performed by sweeping the frequencies in the first electrode, and then the other. The results show similarity in

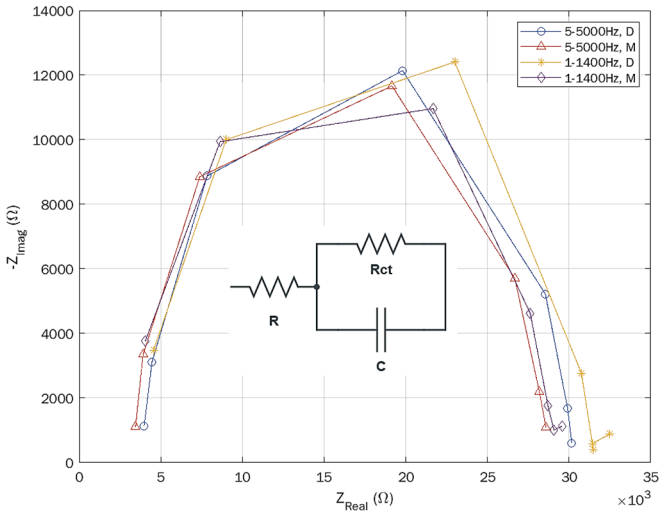

Fig. 5. Experimental data analysis for extracting charge transfer resistance (R_{ct}) in the range of using 5 – 5000 Hz and 1-1400 Hz using the proposed device (D) and Autolab potentiostat Metrohm (M), respectively.

high frequencies with more errors at low frequencies. Finally, the equivalent electrical circuits depicted comparable values. We noticed the PGSTAT204 device, after several tests, showed an increment in one of the equivalent resistors (R2), but our system still presented the same values, this could be due to the use of the same electrodes several times.

C. Clinical Procedures and Tests

The proposed sensing platform was exposed to various analyses including Ab, BSA, and target protein, then the measured data were used to extract R_{ct} as described in the last sub-section. Herein, the sample preparation is briefly explained and the measurement results demonstrated in Fig. 6 are discussed.

1) Clinical Sample Testing Experimental Procedure: To proceed with testing the performance of the read-out system in the successful implementation of EIS measurement for clinical samples, we have obtained nasopharyngeal swab samples, in UTM from Alberta Public Health Laboratory (Alberta Precision Laboratories, Calgary, AB). Positive and negative samples were validated against quantitative reverse transcription-polymerase chain reaction (qRT-PCR) for containing the SARS-CoV-2 specific genome. The clinical specimens were not treated in any form, including lysing, filtering, purifying, or heat-treatment. The immunosensors were prepared as mentioned in section III. In brief, both working electrodes of the bio-ready strips were incubated with 3 μL of the 50 μg/mL antibody prepared in PBS 1X matrix, for 1 hour at room temperature, and then overnight in a 4°C refrigerator. The strips were then rinsed, dried, and coated with a BSA blocking agent for the elimination of non-specific binding, and rinsed after 30 minutes of incubation at room temperature. The insulating mask was placed on the dried electrodes to create the electrode areas that should be in contact with the redox. As for the clinical sample testing, working electrodes were cast-coated with the clinical samples, incubated at room temperature for 15 minutes, rinsed, and dried. The strips were

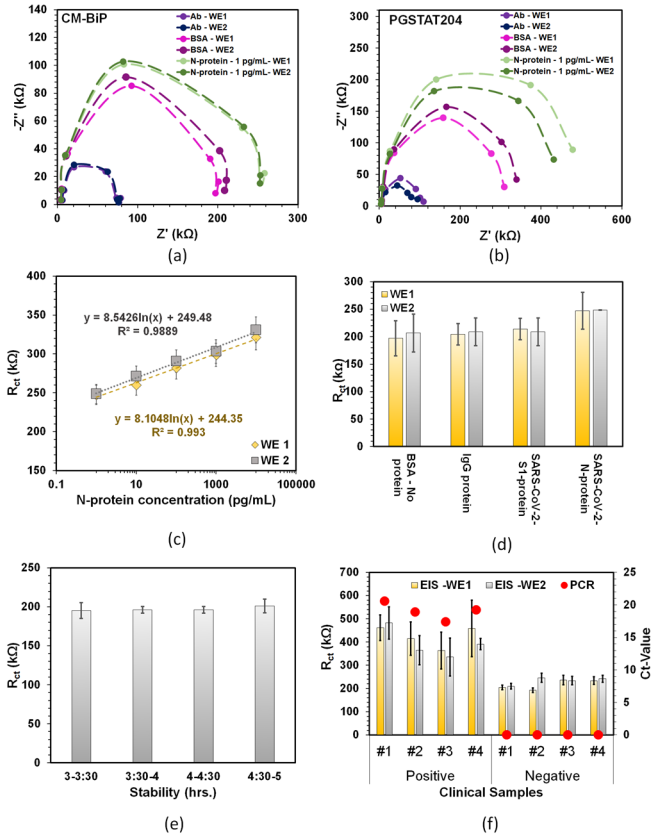

Fig. 6. Electrochemical characterization of the immunosensor using the (a) CM-BiP potentiostat in this study and (b) the commercialized PGSTAT204. (c) Calibration curve depicting the correlation various protein concentrations in spiked solutions versus the CM-BiP EIS response. (d) Selectivity assessment of the immunosensor when incubated with SARS-CoV-2 Spike protein (S1), and Human Immunoglobulin G (IgG), compared to the N-protein. (e) Stability tests performed from 3 to 5 hours after assay opening at room temperature. (f) Clinical test result. Error bars are associated with three replicates.

then plugged into the read-out system, for preliminary tests, we introduced the potassium ferri/ferrocyanide (III) redox solution. To comply with the ethical considerations and safety protocols established by the University of Calgary (Ethics ID: REB20-1032), all experimental procedures involving the handling and testing of the clinical samples were performed by trained personnel in a virology-specialized laboratory under Class II Biosafety Cabinet. The waste materials were safely handled according to safety protocol, and the read-out system was sanitized using UV rays in the safety cabinet after each experiment.

2) Electrochemical Characterization of Clinical Samples: The functionality of the read-out system was further validated by comparing the obtained Nyquist plots associated with the stepwise surface modifications, extracted using the custom-made bipotentiostat (CM-BiP) (Fig. 6 (a)), and commercial PGSTAT204 (Fig. 6 (b)). The graphs illustrate the capability of the read-out system in tracking the increase in the R_{ct}, caused by additional layers of bioanalytes, antibodies, BSA, and ultimately the interaction with the target protein. This trend has been the expectation from the developed readout system as the commercial potentiostat also tracks the changes

in the R_{ct} value in the stepwise modification of the surface, as depicted by the increase in the diameter of the Nyquist diagrams. To better illustrate the potential of the system in quantifiably measuring the concentrations of the target analyte, N-protein, in spiked PBS solution, we also tested the immunosensor under incubation with standard concentrations, which resulted in the calibration curve (Fig. 6 (c)) relating the signal of each concentration to EIS response obtained from CM-BiP system. The calibration curve depicts a strong similarity between the two working electrodes in detecting the protein within a similar concentration range, with a sensitivity of 2936.52 $\Omega \cdot$ mL/pg $\cdot$ mm^2 for WE1, and 3095.14 $\Omega \cdot$ mL/pg $\cdot$ mm^2 for WE2. The selective response of the platform was also investigated when incubating the immunosensors immobilized with N-protein antibodies, with S1 protein and IgG, showing that there is no significant difference between the IgG and S1 incubated electrodes, with the BSA blank signal Fig. 6 (d). To prove the stable conjugation of the antibodies on the surface of the bio-ready electrodes, the strips incubated with COVID-19 negative clinical samples were tested in a time window between 3 to 5 hours after assay opening, showing consistent results, and confirming that the system is stable at least for 5 hours at room temperature (Fig. 6 (e)). Also, the system was tested using four positive, and four negative clinical specimens, and as demonstrated in Fig. 6 (f), the read-out system could successfully detect and differentiate specimens obtained from infected individuals. The readout platform was reproducible when testing three different boards with an RSD of 6.91% for WE1 and 8.03% for WE2.

VI. Conclusion

In this paper, we presented a new handheld impedance-based biosensing platform for the detection of the SARS-CoV-2 specific antigen biomarker. The proposed system features an out system, specifically designed for compatible signal acquisition from a disposable dual-biosensor. The read-out platform was successfully implemented, characterized, and tested, likewise the performance of the platform in terms of distinguishing impedance change associated with exposure of the immunosensor to clinical samples, or spiked antigen solutions was further evaluated, showing sensitive and reliable results. The results obtained from stepwise surface modification on the sensor were compared with standard commercialized bi-potentiostat to prove the functionality and applicability of the proposed read-out system. The proposed platform offers a one-of-a-kind impedance-based bi-potentiostat, in terms of its instrumental simplicity, noise-less signal generation and acquisition, compactness, and inexpensiveness. The system is advantageous for situations such as a pandemic, as it is low-cost ($80 compared to more than $1000 commercial potentiostats) and can be urgently produced, can detect low amounts of proteins, and the multiplexing feature allows for the detection of different biomarkers, possibly one from other similar infectious diseases for more accurate disease diagnosis. Although the system could successfully and reliably detect the protein in both spiked and clinical samples, there is room for further enhancement for decreasing the limit of detection, in terms of embedding more advanced noise cancelation systems, using a curve-fitting method for obtaining the Nyquist plots and determining the R_{ct}, and performing the immunoassay preparation steps automatically using automated sampling techniques, for reducing the user errors, and adding to the assay's precision. The integrated system proved to perform as a reliable, accurate, and cost-effective point-of-care technology companion for COVID-19 rapid testing and other possible pandemic situations in the future.

Acknowledgment

The authors would like to thank the Alberta Public Health Laboratory in Calgary and their research staff members LeeAnn Turnbull and Kanti Pabbaraju for their support in providing access to clinical samples.

Giancarlo Ayala-Charca, Deniz Sadighibayan, and Ebrahim Ghafar-Zadeh are with the Biologically Inspired Sensors and Actuators, Department of Electrical Engineering and Computer Science, Lassonde School of Engineering, York University, Toronto, ON M3J1P3, Canada (e-mail: gcayala@yorku.ca; demizdg@yorku.ca; egz@yorku.ca).

Razieh Salahandish is with the BioMEMS and Bioinspired Microfluidic Laboratory, Department of Mechanical and Manufacturing Engineering, University of Calgary, Calgary, AB T2N 1N4, Canada, and also with the Center for Bioengineering Research and Education, University of Calgary, Calgary, AB T2N 1N4, Canada (e-mail: razieh.salahandish@ucalgary.ca).

Mahmood Khalghollah is with the BioMEMS and Bioinspired Microfluidic Laboratory, Department of Mechanical and Manufacturing Engineering, University of Calgary, Calgary, AB T2N 1N4, Canada, and also with the Department of Electrical and Software Engineering, University of Calgary, Calgary, AB T2N 1N4, Canada (e-mail: mahmood.khalghollah@ucalgary.ca).

Fatemeh Haghayegh is with the BioMEMS and Bioinspired Microfluidic Laboratory, Department of Mechanical and Manufacturing Engineering, University of Calgary, Calgary, AB T2N 1N4, Canada (e-mail: fatemeh.haghayegh@ucalgary.ca).

Amir Sanati-Nezhad is with the BioMEMS and Bioinspired Microfluidic Laboratory, Department of Mechanical and Manufacturing Engineering, University of Calgary, Calgary, AB T2N 1N4, Canada, also with the Center for Bioengineering Research and Education, University of Calgary, Calgary, AB T2N 1N4, Canada, and also with the Biomedical Engineering Graduate Program, University of Calgary, Calgary, AB T2N 1N4, Canada (e-mail: amir.sanatinezhad@ucalgary.ca).

References

[1] H. Li, S.-M. Liu, X.-H. Yu, S.-L. Tang, and C.-K. Tang, "Coronavirus disease 2019 (COVID-19): Current status and future perspectives," *Int. J. Antimicrobial Agents*, vol. 55, no. 5, May 2020, Art. no. 105951, doi: 10.1016/j.ijantimicag.2020.105951.

[2] C. E. Gómez, B. Perdiguero, and M. Esteban, "Emerging SARS-CoV-2 variants and impact in global vaccination programs against SARS-CoV-2/COVID-19," *Vaccines*, vol. 9, no. 3, p. 243, Mar. 2021, doi: 10.3390/vaccines9030243.

[3] *WHO Director-General's Opening Remarks at the Media Briefing on COVID-19—16 March 2020*. Accessed: Apr. 13, 2022. [Online]. Available: https://www.who.int/director-general/speeches/detail/who-director-general-s-opening-remarks-at-the-media-briefing-on-covid-19—16-march-2020

[4] M. Osman, T. Klopfenstein, N. Belfeki, V. Gendrin, and S. Zayet, "A comparative systematic review of COVID-19 and influenza," *Viruses*, vol. 13, no. 3, p. 452, Mar. 2021, doi: 10.3390/v13030452.

[5] L. Xu, D. Li, S. Ramadan, Y. Li, and N. Klein, "Facile biosensors for rapid detection of COVID-19," *Biosensors Bioelectron.*, vol. 170, Dec. 2020, Art. no. 112673, doi: 10.1016/j.bios.2020.112673.

[6] D. Sadighbayan and E. Ghafar-Zadeh, "Portable sensing devices for detection of COVID-19: A review," *IEEE Sensors J.*, vol. 21, no. 9, pp. 10219–10230, May 2021, doi: 10.1109/JSEN.2021.3059970.

[7] F. J. C. González *et al.*, "Utility of lateral flow tests in SARS-CoV-2 infection monitorization," *Revista Española de Quimioterapia*, vol. 33, no. 4, pp. 258–266, Jul. 2020, doi: 10.37201/req/052.2020.

[8] W.-Y. Hsieh *et al.*, "Development and efficacy of lateral flow point-of-care testing devices for rapid and mass COVID-19 diagnosis by the detections of SARS-CoV-2 antigen and Anti-SARS-CoV-2 antibodies," *Diagnostics*, vol. 11, no. 10, p. 1760, Sep. 2021, doi: 10.3390/diagnostics11101760.

[9] P. Damborsky, J. Švitel, and J. Katrlik, "Optical biosensors," *Essays Biochem.*, vol. 60, no. 1, pp. 91–100, 2016, doi: 10.1042/ebc20150010.

[10] D. Grieshaber, R. MacKenzie, J. Vörös, and E. Reimhult, "Electrochemical biosensors–sensor principles and architectures," *Sensors*, vol. 8, no. 3, pp. 1400–1458, Mar. 2008, doi: 10.3390/s80314000.

[11] C. Margo, J. Katrib, M. Nadi, and A. Rouane, "A four-electrode low frequency impedance spectroscopy measurement system using the AD5933 measurement chip," *Physiol. Meas.*, vol. 34, no. 4, pp. 391–405, Apr. 2013, doi: 10.1088/0967-3334/34/4/391.

[12] P. Chandra, "Miniaturized label-free smartphone assisted electrochemical sensing approach for personalized COVID-19 diagnosis," *Sensors Int.*, vol. 1, Jan. 2020, Art. no. 100019, doi: 10.1016/j.sintl.2020.100019.

[13] J. Kudr, P. Michalek, L. Ilieva, V. Adam, and O. Zitka, "COVID-19: A challenge for electrochemical biosensors," *TrAC Trends Anal. Chem.*, vol. 136, Mar. 2021, Art. no. 116192, doi: 10.1016/j.trac.2021.116192.

[14] S. S. Mahshid, S. E. Flynn, and S. Mahshid, "The potential application of electrochemical biosensors in the COVID-19 pandemic: A perspective on the rapid diagnostics of SARS-CoV-2," *Biosensors Bioelectron.*, vol. 176, Mar. 2021, Art. no. 112905, doi: 10.1016/j.bios.2020.112905.

[15] E. Cesewski and B. N. Johnson, "Electrochemical biosensors for pathogen detection," *Biosensors Bioelectron.*, vol. 159, Jul. 2020, Art. no. 112214, doi: 10.1016/j.bios.2020.112214.

[16] H. S. Magar, R. Y. A. Hassan, and A. Mulchandani, "Electrochemical impedance spectroscopy (EIS): Principles, construction, and biosensing applications," *Sensors*, vol. 21, no. 19, p. 6578, Oct. 2021, doi: 10.3390/s21196578.

[17] L.-V. Kiew *et al.*, "Development of flexible electrochemical impedance spectroscopy-based biosensing platform for rapid screening of SARS-CoV-2 inhibitors," *Biosensors Bioelectron.*, vol. 183, Jul. 2021, Art. no. 113213, doi: 10.1016/j.bios.2021.113213.

[18] M. Z. Rashed *et al.*, "Rapid detection of SARS-CoV-2 antibodies using electrochemical impedance-based detector," *Biosensors Bioelectron.*, vol. 171, Jan. 2021, Art. no. 112709, doi: 10.1016/j.bios.2020.112709.

[19] S. A. Perdomo *et al.*, "SenSARS: A low-cost portable electrochemical system for ultra-sensitive, near real-time, diagnostics of SARS-CoV-2 infections," *IEEE Trans. Instrum. Meas.*, vol. 70, pp. 1–10, 2021, doi: 10.1109/TIM.2021.3119147.

[20] L. Fabiani *et al.*, "Magnetic beads combined with carbon black-based screen-printed electrodes for COVID-19: A reliable and miniaturized electrochemical immunosensor for SARS-CoV-2 detection in saliva," *Biosensors Bioelectron.*, vol. 171, Jan. 2021, Art. no. 112686, doi: 10.1016/j.bios.2020.112686.

[21] R. Nandeshwar, M. S. Kumar, K. Kondabagil, and S. Tallur, "Electrochemical immunosensor platform using low-cost ENIG PCB finish electrodes: Application for SARS-CoV-2 spike protein sensing," *IEEE Access*, vol. 9, pp. 154368–154377, 2021, doi: 10.1109/ACCESS.2021.3128668.

[22] S. Mahari, A. Roberts, D. Shahdeo, and S. Gandhi, "eCovSens-ultrasensitive novel in-house built printed circuit board based electrochemical device for rapid detection of nCovid-19," *Biorxiv*, vol. 2020, Jan. 2020, Art. no. 059204, doi: 10.1101/2020.04.24.059204.

[23] A. Raziq, A. Kidakova, R. Boroznjak, J. Reut, A. Öpik, and V. Syritski, "Development of a portable MIP-based electrochemical sensor for detection of SARS-CoV-2 antigen," *Biosensors Bioelectron.*, vol. 178, Apr. 2021, Art. no. 113029, doi: 10.1016/j.bios.2021.113029.

[24] Y. Huang, C. Yang, X.-F. Xu, W. Xu, and S.-W. Liu, "Structural and functional properties of SARS-CoV-2 spike protein: Potential antivirus drug development for COVID-19," *Acta Pharmacologica Sinica*, vol. 41, no. 9, pp. 1141–1149, Sep. 2020, doi: 10.1038/s41401-020-0485-4.

[25] T. Gao *et al.*, "Identification and functional analysis of the SARS-COV-2 nucleocapsid protein," *BMC Microbiol.*, vol. 21, no. 1, p. 58, Dec. 2021, doi: 10.1186/s12866-021-02107-3.

[26] S. Shin Low *et al.*, "Smartphone-based portable electrochemical biosensing system for detection of circulating microRNA-21 in saliva as a proof-of-concept," *Sens. Actuators B, Chem.*, vol. 308, Apr. 2020, Art. no. 127718, doi: 10.1016/j.snb.2020.127718.

[27] W. Zhao, S. Tian, L. Huang, K. Liu, L. Dong, and J. Guo, "A smartphone-based biomedical sensory system," *Analyst*, vol. 145, no. 8, pp. 2873–2891, Apr. 2020, doi: 10.1039/c9an02294e.

[28] M. A. Ehsan, S. A. Khan, and A. Rehman, "Screen-printed graphene/carbon electrodes on paper substrates as impedance sensors for detection of coronavirus in nasopharyngeal fluid samples," *Diagnostics*, vol. 11, no. 6, p. 1030, Jun. 2021, doi: 10.3390/diagnostics11061030.

[29] A. Ramanujam, S. Almodovar, and G. G. Botte, "Ultra-fast electrochemical sensor for point-of-care COVID-19 diagnosis using non-invasive saliva sampling," *Processes*, vol. 9, no. 7, p. 1236, Jul. 2021. [Online]. Available: https://www.mdpi.com/2227-9717/9/7/1236

[30] M. S. Kumar *et al.*, "Electrochemical sensing of SARS-CoV-2 amplicons with PCB electrodes," *Sens. Actuators B, Chem.*, vol. 343, Sep. 2021, Art. no. 130169, doi: 10.1016/j.snb.2021.130169.

[31] T. Chaibun *et al.*, "Rapid electrochemical detection of coronavirus SARS-CoV-2," *Nature Commun.*, vol. 12, no. 1, p. 802, Dec. 2021, doi: 10.1038/s41467-021-21121-7.

[32] Y. Yuan *et al.*, "A Fe3O4@Au-basedpseudo-homogeneous electrochemical immunosensor for AFP measurement using AFP antibody-GNPs-HRP as detection probe," *Anal. Biochemistry*, vol. 534, pp. 56–63, Oct. 2017, doi: 10.1016/j.ab.2017.07.015.

[33] J. Bhardwaj, S. Devarakonda, S. Kumar, and J. Jang, "Development of a paper-based electrochemical immunosensor using an antibody-single walled carbon nanotubes bio-conjugate modified electrode for label-free detection of foodborne pathogens," *Sens. Actuators B, Chem.*, vol. 253, pp. 115–123, Dec. 2017, doi: 10.1016/j.snb.2017.06.108.

[34] *AD5933: Impedance Converter*. Accessed: May 1, 2022. [Online]. Available: https://www.analog.com/media/en/technical-documentation/data-sheets/AD5933.pdf

[35] *nRF52840: RF System on a Chip*. Accessed: May 1, 2022. [Online]. Available: https://infocenter.nordicsemi.com/pdf/nRF52840_PS_v1.7.pdf

[36] *24LC256: 256-Kbit I2C Serial EEPROM*. Accessed: May 1, 2022. [Online]. Available: https://ww1.microchip.com/downloads/en/DeviceDoc/24AA256-24LC256-24FC256-256-Kbit-I2C-Serial-EEPROM-20001203X.pdf

[37] *DS1077Lx-40: Programmable Oscillator*. Accessed: May 1, 2022. [Online]. Available: https://datasheets.maximintegrated.com/en/ds/DS1077L.pdf

[38] *SparkFun Pro nRF52840 Mini—Bluetooth Development Board*. Accessed: May 1, 2022. [Online]. Available: https://www.sparkfun.com/products/15025

[39] L. Breniuc, V. David, and C.-G. Haba, "Wearable impedance analyzer based on AD5933," in *Proc. Int. Conf. Expo. Electr. Power Eng. (EPE)*, Oct. 2014, pp. 585–590, doi: 10.1109/ICEPE.2014.6969977.

[40] J. Ferreira, F. Seoane, and K. Lindecrantz, "AD5933-based electrical bioimpedance spectrometer. Towards textile-enabled applications," in *Proc. Annu. Int. Conf. IEEE Eng. Med. Biol. Soc.*, Aug. 2011, pp. 3282–3285, doi: 10.1109/IEMBS.2011.6090891.

[41] M. Simic, "Realization of complex impedance measurement system based on the integrated circuit AD5933," in *Proc. 21st Telecommun. Forum Telfor (TELFOR)*, Nov. 2013, pp. 573–576, doi: 10.1109/TELFOR.2013.6716294.

[42] X. Liu, C. Cheng, J. Wu, S. Eda, and Y. Guo, "A low cost and palm-size analyzer for rapid and sensitive protein detection by AC electrokinetics capacitive sensing," *Biosensors Bioelectron.*, vol. 90, pp. 83–90, Apr. 2017, doi: 10.1016/j.bios.2016.10.098.

[43] K. Chabowski, T. Piasecki, A. Dzierka, and K. Nitsch, "Simple wide frequency range impedance meter based on AD5933 integrated circuit," *Metrol. Meas. Syst.*, vol. 22, no. 1, pp. 13–24, Mar. 2015, doi: 10.1515/mms-2015-0006.

[44] *Library Code for AD5933*. Accessed: May 1, 2022. [Online]. Available: https://github.com/WuMRC/drive

[45] *Impedance Spectroscopy Using the AD5933*. Accessed: May 1, 2022. [Online]. Available: https://circuitcellar.com/research-design-hub/impedance-spectroscopy-using-the-ad5933/

[46] V. Rasalingam, "A system for electrochemical impedance spectroscopy of electrochemical sensors," Dept. Elect. Electron. Eng., Imperial College London, London, U.K., 2018.

[47] M. Usach, "How to configure the AD5933/AD5934," Analog Devices, Cambridge, MA, USA, 2013. [Online]. Available: https://www.analog.com/media/en/technical-documentation/application-notes/AN-1252.pdf

Giancarlo Ayala-Charca (Member, IEEE) received the B.Sc. degree in electronics engineering from the National University of Engineering, Lima, Peru, the M.Eng. degree in biomedical engineering from Polytechnique Montréal, Montréal, and the M.A.Sc. degree in computer engineering from York University, Toronto, ON, Canada. He is currently a Research Associate with the Biologically Inspired Sensors and Actuators (BioSA) Laboratory, York University. His research interests include electrochemical and photonic biosensors, bio-MEMS, microelectronics, mixed-signal design, embedded systems, and SoC.

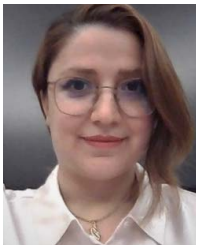

Razieh Salahandish received the dual Ph.D. degree from the BioMEMS Laboratory and IUST for the development of different nano-biosensor. She specializes in electrochemical biosensors and has worked on projects related to the detection of cancer, Hepatitis C and B, Influenza, cardiovascular, brain injuries, SARS-CoV-2, and neurodegenerative diseases. She has been the Senior Scientist and the Co-Founder of Criticare Dx and Electrody. She is currently a Senior Research Assistant and a Canadian Institute for Health Research (CIHR) Postdoctoral Fellow with the BioMEMS and Bioinspired Laboratory, University of Calgary, working on multiplexed microfluidic-based nano biosensors for rapid disease detection and point-of-care integrated diagnostic systems.

Mahmood Khalghollah (Graduate Student Member, IEEE) received the B.Sc. and M.Sc. degrees in mechanical engineering from Shiraz University. He is pursuing the dual Ph.D. degree with the Department of Electrical and Software Engineering, University of Calgary and LSIH. He is also a Graduate Research Assistant with the Department of Electrical and Software Engineering, University of Calgary and LSIH. His current research interests include design automation of LOC, AI system development, and advanced control design.

Deniz Sadighbayan received the B.Sc. degree in applied chemistry from the University of Tabriz in 2017 and the M.Sc. degree in medical nanotechnology from the Tabriz University of Medical Sciences in 2019. She is pursuing the Ph.D. degree with the Biologically Inspired Sensors and Actuators Laboratory (BioSA), Faculty of Science, Department of Biology, York University. She is interested in designing nano bio-sensors for disease detection, point-of-care devices, and lab-on-a-chip (LOC) technology, and has worked on developing novel nano-immunosensors for ultra-sensitive detection of gastrin-glycine using recombinant antibody fragments. She has published review papers in the field of electrochemical and FET-based biosensors for detecting diseases' biomarkers and is currently working on designing a portable biosensor for the early detection of COVID-19. She has received the Elia Scholars Program Award, the York Graduate Scholarship from York University, and many publication awards from the Pharmaceutical Analysis and Drug Applied Research Centers.

Fatemeh Haghayegh received the B.Sc. degree in mechanical engineering from the Isfahan University of Technology (IUT), and the M.Sc. degree from the University of Calgary. She is currently a Technical Research Assistant at BioMEMS and Bioinspired Microfluidics. As a Biomedical Researcher, she has the experience of working on the development of a retinal tissue model on microfluidic chips, through her internship with the Royan Institute for Biotechnology, Isfahan, Iran. She has been developing automated capillary microfluidics systems integrated electrochemical immunosensors for COVID-19 detection as her master research.

Amir Sanati-Nezhad received the Ph.D. degree from the Optical Bio-Microsystems Laboratory, Mechanical and Industrial Engineering, Concordia University, Montreal, QC, Canada, in 2013. He is an Associate Professor with the Department of Biomedical Engineering, University of Calgary, and the Canada Research Chair of BioMEMS. He did two years of postdoctoral research with the Department of Biomedical Engineering, McGill University and Harvard—MIT Health Sciences and Technology, from 2013 to 2015. His current research interests include Bio-MEMS, biosensors, bioinspired microfluidics, lab-on-a-chip, and tissue engineering.

Ebrahim Ghafar-Zadeh (Senior Member, IEEE) received the B.Sc. degree in electrical engineering from the KNT University of Technology, Tehran, Iran, the M.Sc. degree in electrical engineering from the University of Tehran, Tehran, and the Ph.D. degree in electrical engineering from the Polytechnique of Montreal, Montreal, Canada, in 2008. His graduate studies focused on complementary metal-oxide-semiconductor (CMOS)-based sensors for lab-on-chip applications. In recognition of his research achievements, he received several fellowship awards, including a Postdoctoral Fellowship (PDF) from the Natural Sciences and Engineering Research Council of Canada (NSERC). Then, he continued his PDF research studies in electrical engineering at McGill University, Montreal, Canada, and bioengineering with the University of California at Berkeley, Berkeley. In 2013, he joined as an Assistant Professor with the Department of Electrical Engineering and Computer Science (EECS), Lassonde School of Engineering, York University, where he is currently an Associate Professor, a member of Graduate Programs of Departments of EECS and Biology, and the Director of the Biologically Inspired Sensors and Actuators (BioSA) Research Laboratory. His research is aimed at exploring novel integrated sensors and actuators for life science applications. Since 2013, Prof. Ghafar-Zadeh has been published more than 100 journals and conference papers and trained more than 40 highly qualified personnel (HQP) in the fields of electrical engineering and biology. He is a Licensed Professional Engineer in Ontario.